Event-Triggered Control for LPV Modeling of DC-DC Boost Converter

Sandeep Kumar Soni, Saumya Singh, Kumar Abhishek Singh, Xiaogang Xiong, R.K. Saket, and Ankit Sachan

***Abstract*—This study presents the event-triggered control (ETC) for linear parameter varying (LPV) model of boost converters. We examine the nonlinear dynamics of boost converters in the LPV framework. The proposed controller is duty-ratio-dependent and provides better performance while requiring less computation. Using the parameter-dependent Lyapunov function (PDLF), we demonstrate the stablity analysis of the proposed approach. Furthermore, we demonstrate that the inter-event time is lower bound by a positive constant, which indicates Zeno behavior free performance. In comparison to earlier time-invariant synthesis techniques, the LPV formulation offers for increased robustness and performance properties. Simulation and experimental results validate the effectiveness of the proposed method.**

***Index Terms*—Linear parameter-varying systems, ETC, boost converter, parameter dependent Lyapunov function**

I. Introduction

SINCE renewable energy has become more prevalent over the past few decades, energy conversion technologies have been facing new challenges [1]. One of these difficulties is that several devices that store or create electrical energy (e.g., batteries [2], ultracapacitors [3], fuel cells [4], and solar panels [5]) are constructed using low-voltage cells, which are frequently coupled in series to get a suitable voltage. The linking of a large number of cells in series increases the system's complexity and may degrade its performance due to cell variances (e.g., manufacturing discrepancies) and varied operating circumstances (e.g., temperature). Furthermore, the output voltage of various sources of electrical energy varies significantly based on a variety of parameters, including the output current, state of charge, and solar radiation. In many applications, such as running electrical motors or injecting power into the grid a reasonably high and consistent voltage is frequently required. When this is the case, a step-up converter can be used to boost the source voltage to the level required by the application while maintaining a constant output voltage despite source voltage fluctuations [6].

The study of step-up converters (boost converters) is therefore crucial and essential. From the control perspective, boost converters exhibit nonlinear dynamics with nonminimal phase behavior [7]. In this article, the nonlinear dynamics of a boost converter is turned into a LPV system and a duty ratio dependent controller is designed. The LPV system is essentially a linear system with a number of time-varying parameters, which allows it to simulate a wide range of physical systems [8], [9]. The tracking control for LPV modeling of boost converters is implemented with interpolation method in [10]. Other notable LPV systems results are presented in [11], [12] and references therein.

The results mentioned above used the continuous deployment of a control signal for LPV systems and boost converters. On the other hand, practical systems require fewer resources, bandwidth and computations. Several studies have utilized the advantages of ETC in this situation [13], [14]. The same event-triggered approach is explored for the nonlinear multiagent systems in [15]. The other remarkable works based on the event-triggered strategy for the estimation problems of Markov jump systems are studied in [16], [17]. As a result of this method's benefits, many researchers have applied it to the problem of voltage regulation in power converters. In [18], an event-triggered PI controller for voltage regulation of a DC-DC buck converter is examined. Recently, an event-triggered approach is presented for microrobot position control in [19]. The same approach is exploited for the missile guidance problem in [20].

Taking the above-mentioned result of boost converters and LPV systems, and integrating the benefits of ETC, we designed an ETC for LPV framework of boost converter. To the best of the authors knowledge, this is the first attempt to design the ETC for LPV modeling of boost converters. The paper's contribution is as follows: (1) We present LPV modeling of boost converters, which is less conservative than time-invariant synthesis. (2) We present a parameter-dependent synthesis approach for generating parameter-dependent controllers that can improve performance such as the disturbance rejection characteristic while maintaining the converter's robustness and damping features. (3) The controller updates when the triggering condition satisfies, otherwise not. (4) We provided a lower bound on the inter-event time to prevent Zeno behavior.

The paper is organised as follows.: A system modeling and problem formulation are described in Section II. The paper's important results are reported in Section III. In Section IV,

*This work was supported in part by Shenzhen Fundamental Research Program under Grants KQTD20190929172545139, GXWD20200803230628015, and GuangDong Research Foundation 2022A1515011521; (Corresponding authors: Xiaogang Xiong, Ankit Sachan)

Sandeep Kumar Soni is with INSA Centre Val de Loire, University d'Orleans, PRISME EA 4229, Bourges Cedex 18022, France, E-mail: sandeep.soni@insa-cvl.fr.

Saumya Singh, and R. K. Saket are with the Department of Electrical Engineering, Indian Institute of Technology(BHU), Varanasi, 221005, U.P. India, E-mail: (saumyasingh.rs.eee20, rksaket.eee)@iitbhu.ac.in

Xiaogang Xiong is with School of Mechanical Engineering and Automation, Harbin Institute of Technology Shenzhen, P. R. China, E-mail: xiongxg@hit.edu.cn.

Kumar Abhishek Singh is with MCCI, Tyndall National Institute, Cork, Ireland, E-mail: Kumar.singh@tyndall.ie

Ankit Sachan is with Graduate School of Advanced Science and Engineering, Hiroshima University, Higashi, Hiroshima, Japan, E-mail: sachan@hiroshima-u.ac.jp

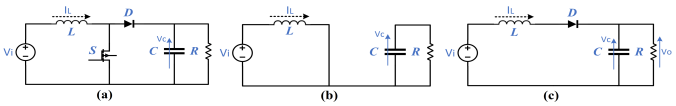

Fig. 1: Boost converter circuit diagram and switching loss: (a) Circuit schematic; (b) Switch is on; (c) Switch is off.

simulation and experimental results are presented. Finally, Section V concludes the article.

Notation: For a function $f(x)$, its upper right Dini derivative is defined by $\mathcal{D}^+ f(x) = \lim_{\tau \to 0^+} \sup\left((f(x+\tau) - f(x))/\tau\right)$.

II. Problem Formulation

A boost converter circuit diagram is shown in Fig. 1(a). The inductor current is represented by I_L, while the capacitor voltage is represented by V_c in this paper. Let $x = \begin{bmatrix} I_L & V_c \end{bmatrix}^T$ is the state variable, $u = V_i$ is the input variable, and $y = \begin{bmatrix} I_L & V_o \end{bmatrix}^T$ is the output variable. When the switch is on and off, the boost converter has two operation states, as shown in Fig. 1(b) and (c).

If the switch (S) is on, as seen in Fig. 1(b), the state-space can be defined as follows:

$$\begin{aligned} \dot{x} &= \begin{bmatrix} 0 & 0 \\ 0 & -\frac{1}{CR} \end{bmatrix} x + \begin{bmatrix} \frac{1}{L} \\ 0 \end{bmatrix} u \triangleq A_1 x + B_1 u \\ y &= \begin{bmatrix} 1 & 0 \\ 0 & 1 \end{bmatrix} x \triangleq C_1 x. \end{aligned} \tag{1}$$

When the switch (S) is turned off, as seen in Fig. 1(c), the state-space form can be written as follows:

$$\begin{aligned} \dot{x} &= \begin{bmatrix} 0 & -\frac{1}{L} \\ \frac{1}{C} & -\frac{1}{CR} \end{bmatrix} x + \begin{bmatrix} \frac{1}{L} \\ 0 \end{bmatrix} u \triangleq A_2 x + B_2 u \\ y &= \begin{bmatrix} 1 & 0 \\ 0 & 1 \end{bmatrix} x \triangleq C_2 x. \end{aligned} \tag{2}$$

Consider the boost converter's duty ratio is $D = T_{on}/T$, where T is the switching period of the switch and T_{on} is the time interval in which the switch is on in switching period. Let $D_1 = D$ and complementary duty ratio $D_2 = 1 - D$. The boost converter's averaged state-space representation [10] can be determined as follows:

$$\begin{aligned} A(D) &\triangleq D_1 A_1 + D_2 A_2, \quad B(D) \triangleq D_1 B_1 + D_2 B_2 \\ C(D) &\triangleq D_1 C_1 + D_2 C_2 \\ &\begin{cases} \dot{x} &= A(D)x + B(D)u \\ y &= C(D)x. \end{cases} \end{aligned} \tag{3}$$

Remark 1: A state-space averaging technique describe the performance of a system for a period of time that is sufficiently long, compared with the switching period. An average state of the system can be calculated by averaging each state-space weight by the time period that each state has in one period.

Based on the system (3), we see that the state-space of the boost converter varies drastically with changes to the duty ratio $D \in (0, 1)$. Furthermore, the equation (3) includes the product of D and the state variables x. Therefore, responses of state-spaces against the change of duty ratio D become nonlinear. The proposed ETC is as follows:

$$u = K\left(D(t_k)\right) x(t_k), \quad \forall t \in [t_k, t_{k+1}), \tag{4}$$

where $K\left(D(t_k)\right) \in \mathbb{R}^{1\times 2}$ is the parameter varying gain matrix to be designed. By substituting the proposed control (4) into the system (3), the closed-loop system becomes

$$\dot{x} = A(D)x + B(D)K(D(t_k))x(t_k). \tag{5}$$

Let us define the time sequence of event-triggered sampling as t_k for x and D for $k \in \mathbb{N}$. Then, the measuring errors for $t \in [t_k, t_{k+1})$ can be defined as follows:

$$e_x \triangleq x(t_k) - x, \quad e_D \triangleq D(t_k) - D. \tag{6}$$

According to (6), (5) can be expressed as

$$\dot{x} = A(D)x + B(D)K\left(e_D + D\right)\left(e_x + x\right). \tag{7}$$

In order to avoid the notaional complexity, we are not writing explicit function .

Definition 1: [11] For the system (7), the function $V(x, D)$ is called the parameter dependent input to state exponentially stable Lyapunov function if there exists positive constant $\lambda, \underline{\mu}, \bar{\mu}, \mu$ with $\underline{\mu} \le \bar{\mu}$ and a function γ which satisfy

$$\begin{aligned} &\frac{\partial V}{\partial x}\left(A(D)x + B(D)K\left(e_D + D\right)\left(e_x + x\right)\right) + \lambda V(x, D) \\ &\qquad \le -\mu\|x\|^2 + \gamma(\|e_D\|)\|e_x\|\|x\|, \\ &\underline{\mu}\|x\|^2 \le V(x, D) \le \bar{\mu}\|x\|^2. \end{aligned}$$

III. Main Results

The key findings of the paper are discussed in this section. The following is a description of the event-triggering scheme presented in this paper:

$$\|e_x\| \ge \frac{\alpha - 2\bar{\rho}\bar{\beta}\sum_{i=1}^{2}\left\{\bar{k}_{ai}\|e_{Di}\|\right\}}{2\bar{\rho}\bar{\beta}\bar{k} + 2\bar{\rho}\bar{\beta}\sum_{i=1}^{2}\left\{\bar{k}_{ai}\|e_{Di}\|\right\}}\|x\| \tag{8}$$

where $e_{D_i} = D_i(t_k) - D_i$ for $i = 1, 2$, and $\sum_{i=1}^{2} D_i = 1$.

When the event condition (8) is true, the control gets updated and provides the desired stability condition

$$\|e_x\| \le \frac{\alpha - 2\bar{\rho}\bar{\beta}\sum_{i=1}^{2}\left\{\bar{k}_{ai}\|e_{Di}\|\right\}}{2\bar{\rho}\bar{\beta}\bar{k} + 2\bar{\rho}\bar{\beta}\sum_{i=1}^{2}\left\{\bar{k}_{ai}\|e_{Di}\|\right\}}\|x\|. \tag{9}$$

The above discussed fact is demonstrated in the following theorem.

Theorem 1: Consider the closed-loop system (7). For a given positive scalars α, λ and matrix $K(D))$ if there exists a positive definite matrix $P(D)$, such that the following inequality holds

$$\begin{aligned} &A^T(D)P(D) + P(D)A(D) + K^T(D)B^T(D)P(D) \\ &\quad + P(D)B(D)K(D) + \dot{P}(D) + \lambda P(D) + \alpha I < 0 \end{aligned} \tag{10}$$

where, $\max_D\{\|P(D)\|\} \le \bar{\rho}$,

$$\max_D\{\|B(D)\|\} \le \bar{\beta}, \qquad \max_D\{\|K(D)\|\} \le \bar{k}$$

$$\max_D\left\{\left\|\int_0^1 \frac{\partial K(z)}{\partial z_i}|_{z_i = D_i + \tau e_{D_i}} d\tau\right\|\right\} \le \bar{k}_{ai}, \quad i = 1, 2.$$

Then, the system (7) is said to be exponentially stable.

Proof. Consider the parameter dependent Lyapunov function as $V(x,D) = x^T P(D)x$. Using upper right Dini derivative, differentiating $V(x,D)$ along solutions x of the system (7) yields

$$\begin{aligned}
&\dot{V}(x,D) + \lambda V(x,D) \\
&= \dot{x}^T P(D)x + x^T P(D)\dot{x} + x^T \dot{P}(D)x + \lambda x^T P(D)x \\
&= 2\left[x^T P(D)\left\{A(D)x + B(D)\left(K(D+e_D)\right)(x+e_x)\right\}\right] \\
&\quad + x^T \dot{P}(D) + \lambda x^T P(D)x, \qquad (11)
\end{aligned}$$

where $K(D+e_D) = K(D) + \sum_{i=1}^{2}\left\{e_{Di}\bar{K}_i(D,e_D)\right\}$, $\bar{K}_i(D,e_D) = \int_0^1 \frac{\partial K(z)}{\partial z_i}|_{z_i = D_i + \tau e_{Di}} d\tau$, $\tau = (0,1)$. Accordingly, we have

$$\begin{aligned}
&\dot{V}(x,D) + \lambda V(x,D) \qquad (12) \\
&= x^T\left[A^T(D)P(D) + P(D)A(D) + K^T(D)B^T(D)P(D)\right. \\
&\quad \left. + P(D)B(D)K(D) + \dot{P}(D) + \lambda P(D)\right]x \\
&\quad + 2x^T P(D)B(D)K(D)e_x + 2x^T P(D)B(D)\times \\
&\quad \left[\sum_{i=1}^{2}\left\{e_{Di}\bar{K}_i(D,e_D)\right\} + \sum_{i=1}^{2}\left\{e_{Di}\bar{K}_i(D,e_D)\right\}\right] \qquad (13) \\
&\leq -\alpha x^T x + 2x^T P(D)B(D)K(D)e_x + 2x^T P(D)B(D) \\
&\quad \times \left[\sum_{i=1}^{2}\left\{e_{Di}\bar{K}_i\right\}x + \sum_{i=1}^{2}\left\{e_{Di}\bar{K}_i\right\}e_x\right]. \qquad (14)
\end{aligned}$$

Earlier defined norm bounds of the known matrices are applied to the inequality (14), which provides

$$\begin{aligned}
&\dot{V}(x,D) + \lambda V(x,D) \leq -\|x\|\Big[\alpha\|x\| - 2\bar{\rho}\bar{\beta}\bar{k}\|e_x\| \\
&- 2\bar{\rho}\bar{\beta}\sum_{i=1}^{2}\left(\left\{\bar{k}_{ai}\|e_{Di}\|\right\}\|x\| + \left\{\bar{k}_{ai}\|e_{Di}\|\right\}\|e_x\|\right)\Big]. \qquad (15)
\end{aligned}$$

From the inequality (15) and stability condition (9), we can show that

$$\dot{V}(x,D) + \lambda V(x,D) < 0. \qquad (16)$$

Accordingly, one can obtain $V \leq V(t_k)e^{-\lambda(t-t_k)}, \forall t \in [t_k, t_{k+1})$. Thus, the system (7) is exponentially stable. ■

A. Analysis of the Inter-event Time

In this section, Zeno phenomenon free study is demonstrated, and the following theorem explains this fact.

Theorem 2: Consider the closed-loop system (7). For any initial value of $x(t_0)$, if there exist positive constants η and $\bar{h}_i > 0$ that satisfy $\sum_{i=1}^{2}\left\{\bar{k}_{ai}\|e_{Di}\|\right\} \leq \eta$ and $\|\dot{D}\| \leq \bar{h}_i$ for $i = 1,2$. Then, the inter-event time $T_k = t_{k+1} - t_k$ is obtained by the event-triggered scheme (8) is lower bounded by the constant

$$\tau = \min\left\{\frac{\eta}{\sum_{i=1}^{2}\left\{\bar{k}_{ai}\ \bar{h}_i\right\}}, T_k\right\} \qquad (17)$$

with

$$T_k = \frac{\bar{\alpha}}{\bar{\beta}^2\bar{k}^2}\left[\ln\left(1 + \frac{\bar{\alpha}}{\bar{\beta}\bar{k}}\right) - \ln\left(1 + \frac{\bar{\alpha}}{\bar{\beta}\bar{k}}\frac{1}{1 + \frac{\alpha - 2\bar{\rho}\bar{\beta}\eta}{2\bar{\rho}\bar{\beta}\bar{k} + 2\bar{\rho}\bar{\beta}\eta}}\right)\right] \qquad (18)$$

$$\begin{aligned}
&\max_{d\in\mathcal{Q}}\{\|A(D)\|\} \leq \bar{\alpha}, \qquad \max_{d\in\mathcal{Q}}\{\|P(D)\|\} \leq \bar{\rho}, \\
&\max_{d\in\mathcal{Q}}\{\|B(D)\|\} \leq \bar{\beta}, \qquad \max_{d\in\mathcal{Q}}\{\|K(D)\|\} \leq \bar{k}, \\
&\max_{d\in\mathcal{Q}}\left\{\left\|\int_0^1 \frac{\partial K(z)}{\partial z_i}|_{z_i = d_i + \tau e_{di}} d\tau\right\|\right\} \leq \bar{k}_{ai}, \quad i = 1,2.
\end{aligned}$$

Proof. From the closed-loop system (7), we have

$$\begin{aligned}
\|\dot{x}\| &\leq \|A(D) + B(D)K(D+e_D)\|\,\|x\| + \|B(D)K(D+e_D)\| \\
&\quad \times \|e_x\| \leq \left(\bar{\alpha} + \bar{\beta}\bar{k}\right)\|x\| + \bar{\beta}\bar{k}\|e_x\|. \qquad (19)
\end{aligned}$$

One can show that

$$\begin{aligned}
&\mathcal{D}^+\left(\frac{\|e_x\|}{\|x\|}\right) = \mathcal{D}^+\frac{\left(e_x^T e_x\right)^{1/2}}{\left(x^T x\right)^{1/2}} \\
&= \frac{\left(e_x^T e_x\right)^{-1/2} e_x^T \dot{e}_x \left(x^T x\right)^{1/2} - \left(x^T x\right)^{-1/2} x^T \dot{x}\left(e_x^T e_x\right)^{1/2}}{x^T x} \\
&\leq \frac{\|e_x\|\ \|\dot{x}\|}{\|e_x\|\ \|x\|} + \frac{\|x\|\ \|\dot{x}\|\ \|e_x\|}{\|x\|\ \|x\|\ \|x\|} = \left(1 + \frac{\|e_x\|}{\|x\|}\right)\frac{\|\dot{x}\|}{\|x\|} \\
&\leq \left(1 + \frac{\|e_x\|}{\|x\|}\right)\left(\bar{\alpha} + \bar{\beta}\bar{k} + \bar{\beta}\bar{k}\frac{\|e_x\|}{\|x\|}\right) \\
&= \bar{\alpha} + \bar{\beta}\bar{k} + \left(\bar{\alpha} + 2\bar{\beta}\bar{k}\right)\frac{\|e_x\|}{\|x\|} + \bar{\beta}\bar{k}\left(\frac{\|e_x\|}{\|x\|}\right)^2. \qquad (20)
\end{aligned}$$

Consider $\xi = \frac{\|e_x\|}{\|x\|}$ and $e_x = 0$ yields $\xi = 0$. Then, we have the estimation $\mathcal{D}^+\xi \leq \bar{\alpha} + \bar{\beta}\bar{k} + \left(\bar{\alpha} + 2\bar{\beta}\bar{k}\right)\xi + \bar{\beta}\bar{k}\xi^2$. Suppose

$$\dot{\phi} \leq \bar{\alpha} + \bar{\beta}\bar{k} + \left(\bar{\alpha} + 2\bar{\beta}\bar{k}\right)\phi + \bar{\beta}\bar{k}\phi^2 \qquad (21)$$

with $\phi_0 = 0$. We reach at $\xi \leq \phi(t,\phi_0)$ by the comparison principle [13].

Lets assume the previous triggering instant is t_k. When $\frac{\|e_x\|}{\|x\|}$ evolves from 0 to $\Gamma_m(\|e_D\|)$, the next trigger will occur under the condition (8). According to the comparison principle, the inter-event time $T_k = t_{k+1} - t_k$ is lower bound by the time that ϕ evolves from 0 to $\Gamma_m(\|e_D\|)$. After solving the differential equation (21), we obtain that

$$T_k = \frac{\bar{\alpha}}{\bar{\beta}^2\bar{k}^2}\left[\ln\left(1 + \frac{\bar{\alpha}}{\bar{\beta}\bar{k}}\right) - \ln\left(1 + \frac{\bar{\alpha}}{\bar{\beta}\bar{k}}\frac{1}{1 + \Gamma_m(\|e_D\|)}\right)\right]. \qquad (22)$$

When $t = t_k$, the equality $\|e_{Di}\| = 0$ holds, which yields $\Gamma(\|e_D\|) = \Gamma_{\max} = \frac{\alpha}{2\bar{\rho}\bar{\beta}\bar{k}} > 0$. There is no trigger at $t = t_k$ because the triggering interval

$$T_k = \frac{\bar{\alpha}}{\bar{\beta}^2\bar{k}^2}\left[\ln\left(1 + \frac{\bar{\alpha}}{\bar{\beta}\bar{k}}\right) - \ln\left(1 + \frac{\bar{\alpha}}{\bar{\beta}\bar{k}}\frac{1}{1 + \frac{\alpha}{2\bar{\rho}\bar{\beta}\bar{k}}}\right)\right] > 0 \qquad (23)$$

must be satisifed. Therefore, there exists a positive constant η satisfying $\sum_{i=1}^{2}\left\{\bar{k}_{ai}\|e_{Di}\|\right\} \leq \delta$, we get $\Gamma(\|e_D\|) \geq \left(\frac{\alpha - 2\bar{\rho}\bar{\beta}\bar{k}_a\eta}{2\bar{\rho}\bar{\beta}\bar{k} + 2\bar{\rho}\bar{\beta}\bar{k}_a\eta}\right) \triangleq \varpi$. Since, the next trigger only occurs when $\|e_x\| = \Gamma(\|e_D\|)\|x\|$, we deduce that next trigger can not happen before the time of $\frac{\|e_x\|}{\|x\|} = \varpi$. The equality $\sum_{i=1}^{2}\left\{\bar{k}_{ai}\|e_{Di}\|\right\} = \eta$ holds when it is at the time t. Using

This article has been accepted for publication in IEEE Transactions on Circuits and Systems--II: Express Briefs. This is the author's version which has not been fully edited and content may change prior to final publication. Citation information: DOI 10.1109/TCSII.2022.3230418

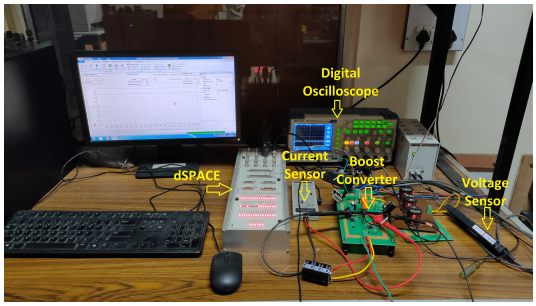

Fig. 2: Hardware setup of the boost converter.

differential mean value theorem [11], one can show that

$$\eta = \sum_{i=1}^{2} \{\bar{k}_{ai} \|e_{Di}\|\} = \sum_{i=1}^{2} \{\bar{k}_{ai} \|D_i - D_i(t_k)\|\} = \sum_{i=1}^{2} \left\{\bar{k}_{ai} \|\dot{D}(\varpi_i)\|\right\} (t - t_k) \leq \sum_{i=1}^{2} \{\bar{k}_{ai} \ \bar{h}_i\} (t - t_k), \quad (24)$$

where $\varpi_i \in (t_k, t)$. Hence, we get $t - t_k \geq \frac{\eta}{\sum_{i=1}^{2} \{\bar{k}_{ai} \ \bar{h}_i\}} > 0$. Employing (22), we can show that $T_k > 0$. Based on (17) and $T_k > 0$, we can demonstrate that the inter-event time is lower bounded by the positive constant. ■

Remark 2: Since, we consider the highest upper bound on the parameter dependent matrices in Theorem 1 and 2, which might offer the conservative results.

IV. NUMERICAL SIMULATION AND EXPERIMENTAL RESULTS

A boost converter with the following specifications: $V_i = 24$V, $V_{\text{ref}} = 48$V, $I_{\text{ref}} = 2$A, $R = 20\Omega$, $L = 1120\mu$H, and $C = 100\mu$F is utilized for the simulation and experimental test. The MATLAB/SIMULINK interface is used to control and acquire data with the dSPACE MicroLabBox. Fig. 2 depicts the hardware arrangement. We examine the controller's performance under two scenarios: (1) output voltage regulation with varying input voltage, and (2) output voltage regulation with variable load. The control input is chosen as $u = u(t_k) = K(D(t_k))x(t_k)$. The design parameters are $K(D) = \begin{bmatrix}0.01 & 0.3\end{bmatrix} + D\begin{bmatrix}0.025 & 0.9\end{bmatrix}$, $D \in (0, 1)$ and scalers are $\alpha = 5, \lambda = 0.7$. They were all chosen to give satisfactory responses.

We compared our results to the results of a related study [18] in order to demonstrate the efficacy of the proposed methodology. For the DC-DC converters in [18], an event-triggered PI controller was designed, and the designed controller was as follows: $u = K_i \int_0^t (V_{\text{ref}} - V_o(t_k))dt + K_p(V_{\text{ref}} - V_o(t_k))$, where $K_p = 0.0175$ and $K_i = 0.5$ are the controller gains.

A. Simulation Results

1) Output voltage regulation with varying input voltage: Variable input voltages are applied to the boost converter while the reference output voltage maintains at 48V. We start with input voltage 21V and increased it to 29V. The output voltage response is illustrated in Fig. 3(a), and the simulation results

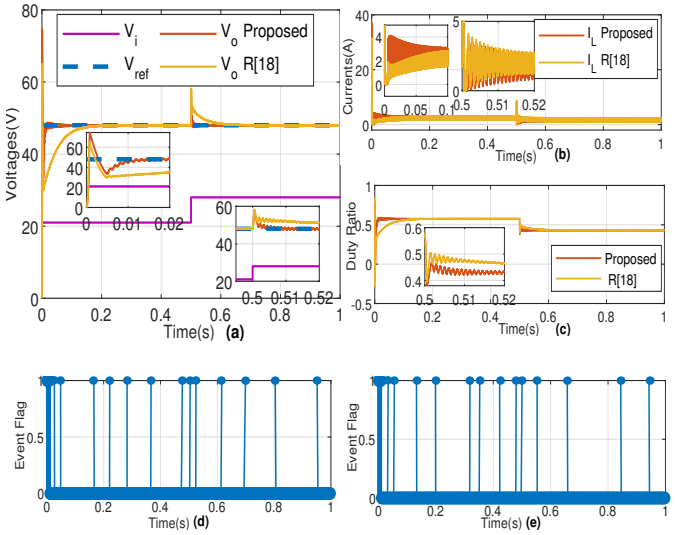

Fig. 3: Simulation response with varying input voltage (21V to 29V): (a) Voltages; (b) Currents; (c) Duty ratio; (d) Proposed event flag; (e) R[18] event flag.

demonstrate that the proposed method reduced the settling time by 60-70% and provided the desired voltage regulation. Furthermore, the proposed approach quickly returns to the required output voltage with the change in input voltage at $t = 0.5s$. In Fig. 3(b), the inductor current response is presented. Fig. 3(c) illustrates the evolution of the control signal, where the duty ratio changes in a zig-zag pattern due to the implementation of ETCs. As shown in Fig. 3(d) and (e), the event flag is set to 1 if the triggering condition is satisfied.

2) Output voltage regulation with varying load: Different load currents are applied to the boost converter while the output voltage is kept at 48V by varying the loads. The initial load current of 2A is gradually raised to 4A. Fig. 4(a) shows the voltage response. As we have seen in previous case, the proposed method reduces the settling time in this one by 60-70% as well. The proposed approach effectively handeled with the load changes at $t = 0.5s$. In Fig. 4(b) the inductor current response is presented. Fig. 4(c) shows how duty ratios evolve with load current. Fig. 4(d) and (e) depicts an event flag that is set to 1 if the triggering condition is satisfied.

B. Experimental Results

The experimental results of the boost converter with the proposed approach are presented in Fig. 5(a) and (b). Fig. 5(a) shows us that when the input voltage changes from 21V to 29V at $t = 0.5s$, while the constant load is kept at $R = 48\Omega$, the output voltage remains around 48V. Similarly, in Fig. 5(b), when the load changes from 48Ω to 24Ω at $t = 0.5s$, while keeping the input voltage constant at $V_i = 21V$, the output voltage remains near 48V. Consequently, the changes in input voltage and load have no effect on the output voltage regulation. In the experimental results of Fig. 5(a) and (b), we can observe oscillations in the output voltage of the converter as a result of the event-triggered nature of the control signal.

According to simulation and experimental results, the introduced technique provides improved steady-state and transient

This article has been accepted for publication in IEEE Transactions on Circuits and Systems--II: Express Briefs. This is the author's version which has not been fully edited and content may change prior to final publication. Citation information: DOI 10.1109/TCSII.2022.3230418

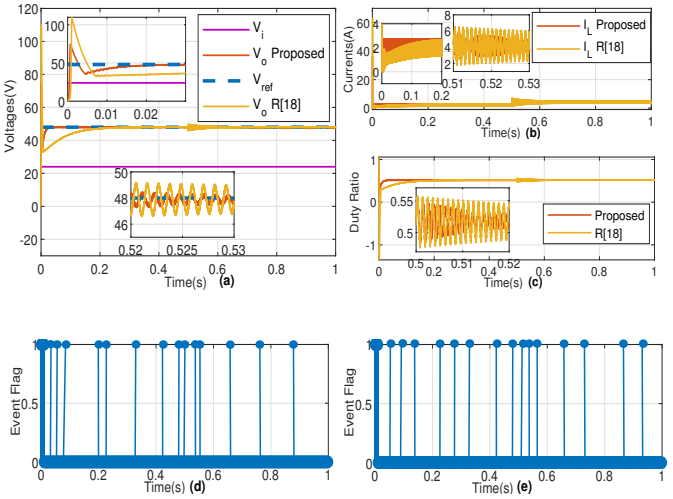

Fig. 4: Simulation response with varying load (48Ω to 24Ω): (a) Voltages; (b) Currents; (c) Duty ratio; (d) Proposed event flag; (e) R[18] event flag.

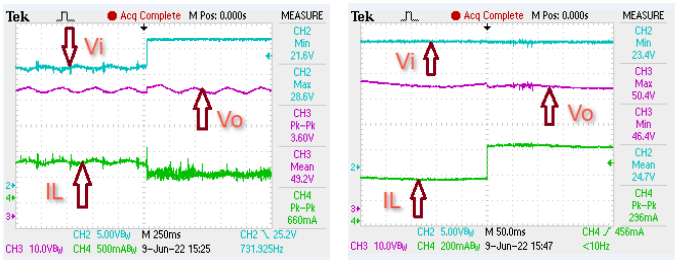

(a) **(b)**

Fig. 5: (a) Experimental response with varying input voltage (21V to 29V); (b) Experimental response with varying load resistor (48Ω to 24Ω).

performance. Therefore, compared to earlier methods, the LPV modeling and event-triggered control synthesis for boost converters provides a number of benefits, including faster dynamics and lower control utilization.

V. CONCLUSION

This paper illustrated an event-triggered control for the LPV framework of a boost converter, including the implementation of an appropriate triggering condition. The controller's duty ratio-dependent design results in enhanced voltage regulation performance. The boost converter and parameter-dependent controller used in the closed-loop system were demonstrated to have stability. The simulation and experimental results for the following scenarios are provided: (i) changing the input voltage; (ii) changing the load currents. In both the scenarios, the controller provided desirable performance while significantly reducing control updates, resulting in minimal use of computational and communication resources. Furthermore, to eliminate Zeno behavior, a lower bound on the inter-event time is provided.

REFERENCES

[1] F.S. Garcia, J.A. Pomilio and G. Spiazzi, "Modeling and control design of the interleaved double dual boost converter," *IEEE Transactions on Industrial Electronics*, vol. 60, no. 8, pp. 3283–3290, 2012.

[2] M.B. Camara, H. Gualous, F. Gustin and A. Berthon, "Design and new control of DC/DC converters to share energy between supercapacitors and batteries in hybrid vehicles," *IEEE Transactions on Vehicular Technology*, vol. 57, no. 5, pp. 2721–2735, 2008.

[3] P.J. Grbovic, P. Delarue, P.L. Moigne and P. Bartholomeus, "Modeling and control of the ultracapacitor-based regenerative controlled electric drives," *IEEE Transactions on Industrial Electronics*, vol. 58, no. 8, pp. 3471–3484, 2011.

[4] N. Agrawal, S. Samanta and S. Ghosh, "Optimal state feedback-integral control of fuel-cell integrated boost converter," *IEEE Transactions on Circuits and Systems II: Express Briefs*, vol. 69, no. 3, pp. 1382–1386, 2022.

[5] K.A. Singh, A. Prajapati and K. Chaudhary, "High gain compact inter-leaved boost converter with reduced voltage stress for PV application," *IEEE Journal of Emerging and Selected Topics in Power Electronics*, vol. 10, no. 4, pp. 4763–4770, 2022.

[6] C.Y. Chan, "Adaptive sliding-mode control of a novel buck-boost converter based on zeta converter," *IEEE Transactions on Circuits and Systems II: Express Briefs*, vol. 69, no. 3, pp. 1307–1311, 2022.

[7] F.A. Villarroel, J.R. Espinoza, M.A. Perez, R.O. Ramirez, C.R. Baier, D. Sbarbaro, J.J. Silva and M.A Reyes, "Stable shortest horizon FCS-MPC output voltage control in non-minimum phase boost-type convert-ers based on input-state linearization," *IEEE Transactions on Energy Conversion*, vol. 36, no. 2, pp. 1378–1391, 2021.

[8] A. Khan, X. Bai, B. Zhang and P. Yan, "Interval state estimator design for linear parameter varying (LPV) systems," *IEEE Transactions on Circuits and Systems II: Express Briefs*, vol. 68, no. 8, pp. 2865–2869, 2021.

[9] B. Sereni, M.A.L. Beteto, E. Assunçao and M.C.M. Teixeira, "Pole placement LMI constraints for stability and transient performance of LPV systems with incomplete state measurement," *Journal of the Franklin Institute*, vol. 359, no. 2, pp. 837–858, 2022.

[10] S. Miyoshi, W. Ohnishi, T. Koseki and M. Sato, "Modified preactuation tracking control for LPV systems with application to boost converters," *21st IFAC World Congress*, vol. 53, no. 2, pp. 7319–7324, 2020.

[11] K. Zhu, D. Ma and J. Zhao, "Event triggered control for a switched LPV system with applications to aircraft engines," *IET Control Theory & Applications*, vol. 12, no. 10, pp. 1505–1514, 2018.

[12] Z. Guangdeng, D. Yang, J. Lam and X. Song, "Fault-tolerant control of switched LPV systems: a bumpless transfer approach," *IEEE/ASME Transactions on Mechatronics*, vol. 27, no. 3, pp. 1436–1446, 2022.

[13] A.K. Behera and B. Bandyopadhyay, "Robust sliding mode control: an event-triggering approach," *IEEE Transactions on Circuits and Systems II: Express Briefs*, vol. 64, no. 2, pp. 146–150, 2017.

[14] S.K. Soni, S. Kumar, S. Wang, A. Sachan, D. Boutat and D. Geha, "Sliding mode event-triggered tracking control for robot manipulators with state constraints," *48th Annual Conference of the IEEE Industrial Electronics Society (IECON)*, pp. 1–6, 2022.

[15] W. Zou, P. Shi, Z. Xiang and Y. Shi, "Consensus tracking control of switched stochastic nonlinear multiagent systems via event-triggered strategy," *IEEE Transactions on Neural Networks and Learning Systems*, vol. 31, no. 3, pp. 1036–1045, 2020.

[16] J. Tao, Z. Xiao, Z. Li, J. Wu, R. Wu, P. Shi and X. Wang, "Dynamic event-triggered state estimation for Markov jump neural networks with partially unknown probabilities," *IEEE Transactions on Neural Networks and Learning Systems*, vol. 33, no. 12, pp. 7438–7447, 2022.

[17] Z. Xiao, Z. Wu and J. Tao, "Asynchronous filtering for Markov jump systems within finite time: A general event-triggered communication," *Communications in Nonlinear Science and Numerical Simulation*, vol. 114, pp. 106634, 2022.

[18] K. Nath, P. Nambisan, A. Yesmin and M.K. Bera, "Event-triggered PI control of buck converter in cyber-physical framework," *IEEE Seventh Indian Control Conference (ICC)*, pp. 159–164, 2021.

[19] S.K. Soni, Z.E. Hamdaoui, S. Wang, D. Boutat, M. Djemai and D. Geha, "Event-triggered sliding mode control to manipulate a microrobot with two-magnet system under input constraint," *16th International Workshop on Variable Structure Systems (VSS)*, pp. 225–230, 2022.

[20] S. Kumar, S.K. Soni, A. Sachan, S. Kamal and B. Bandyopadhyay, "Adaptive super-twisting guidance law: an event-triggered approach," *16th International Workshop on Variable Structure Systems (VSS)*, pp. 190–195, 2022.